*Current Research (2025) Newfoundland and Labrador Department of Industry, Energy and Technology Geological Survey, Report 25-1, pages 105-114*

# PRELIMINARY RESULTS OF SATELLITE MULTISPECTRAL-SUPPORTED BEDROCK MAPPING IN NORTHERN LABRADOR

D. Diekrup, A.M. Hinchey, G.W. Sparkes[1], H.E. Campbell[2], L.G. Scorsolini and M. Schofield[1]
Regional Geology Section
[1]Mineral Deposits Section
[2]Terrain Sciences and Geoscience Data Management Section

## ABSTRACT

*The geometry, lithologies and location of the boundary between the Archean Hopedale block and the Proterozoic Southeastern Churchill Province remains poorly constrained and is the focus of an extensive multi-year, multidisciplinary field-mapping project. Given the remote and difficult-to-access study area in UTM grids 13N/05 and 06, satellite multispectral data was utilized to generate remote predictive maps of key mineralogical assemblages and lithologic contacts. This approach is intended to complement and enhance traditional field-based geological mapping efforts. While historically used in arid regions, high-resolution WorldView-3 satellite multispectral data, enhanced by advanced filtering and processing methods, enabled the identification of lithologic variability despite challenging surface conditions.*

*Maxar Technology's WorldView-3 satellite data currently provides the best spatial and spectral resolution available, overcoming the limitations posed by outcrop availability and atmospheric conditions. The resulting remote predictive bedrock map delineates several mineralogical assemblages, identifying surfaces with elevated iron hydroxides, and hydrous and aluminum hydroxide-bearing minerals. These mineral groups can serve as proxies for lithologies and their contacts, often correlating with existing geological map unit boundaries while also revealing discrepancies that require additional investigation. Notable findings include sections of the Nain Plutonic Suite and previously undifferentiated orthogneisses east of the Tasiuyak complex, where multispectral data suggests greater lithologic complexity than currently indicated by field mapping. Additional refinements to geologic contact locations are also highlighted.*

*This study demonstrates the potential of satellite multispectral data in remote geological mapping in north-central Labrador, improving fieldwork efficiency while refining remote predictive maps through ground-truthing. Future efforts will focus on refining the spectral analysis using representative samples including weathered surfaces and acquiring data under optimal atmospheric conditions to enhance processing outcomes.*

## INTRODUCTION

A multi-year mapping initiative investigating the geology of the Hopedale block and the Torngat orogen, which marks the boundary with the Southeastern Churchill Province (Figure 1). Due to the remote and geological complexity of the area, remote-sensing techniques, such as geophysical surveys and multispectral satellite data provide valuable supplemental information. Whilst satellite multispectral data is commonly used in arid regions for the identification of hydrothermal alteration features (*e.g.*, Di Tommaso and Rubinstein, 2007; van der Meer *et al.*, 2012; Kruse *et al.*, 2015; Pour *et al.*, 2019), surface conditions in central Labrador presents challenges for these types of applications. These challenges stem from limited outcrop availability, widespread till and lichen cover on bedrock, as well as vegetation and variable atmospheric conditions, including cloud cover and haze (seasonal) from wildfires. Additionally, publicly available multispectral datasets (*e.g.*, ASTER, Sentinel-2) offer limited spatial (15–90 m) and spectral resolution, limiting their effectiveness in detecting mineralogical variations in exposed bedrock. However, recent work by Sparkes *et al.* (2023) demonstrated the potential of commercially available, high-resolution satellite multispectral data for mapping hydrothermal alteration features in the Long Harbour Group on the south coast of Newfoundland. This study extends that approach to parts of central Labrador, utilizing WorldView-3 data acquired through the European Space Agency under the Geological Survey of Newfoundland and Labrador project "WorldView-3 Supported Bedrock Mapping in Remote Areas of Labrador (PP0097103)." The WorldView-3 system

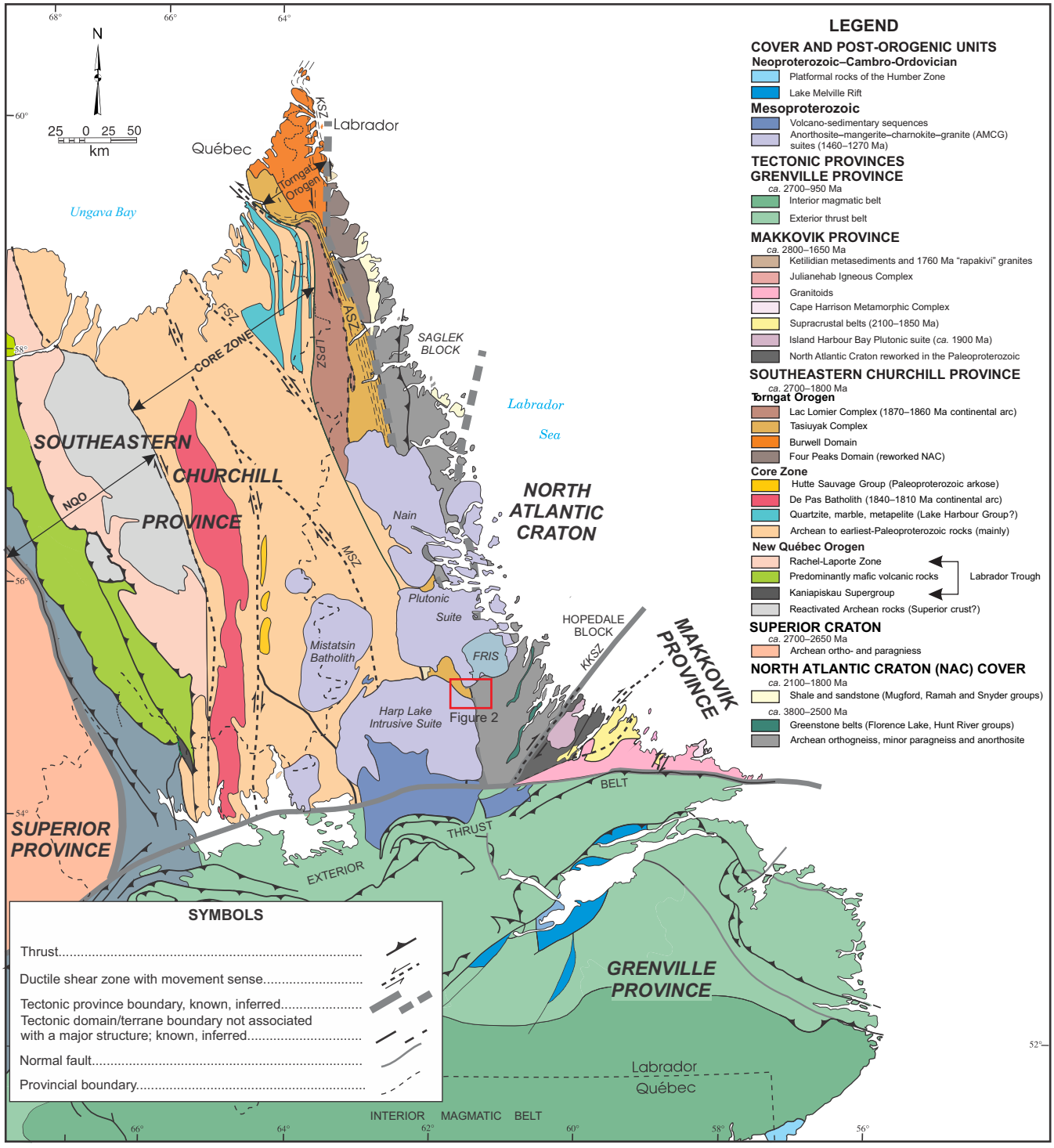


**Figure 1.** *Simplified geologic map of Labrador (after Hinchey* et al.*, 2024). Location of the project area on the boundary between the Hopedale block and Southeastern Churchill Province highlighted by the red box. ASZ=Abloviak shear zone; FSZ=Falcoz shear zone; MSZ= Moonbase shear zone; LPSZ=Lake Pilliamet shear zone; KSZ=Komaktorvik shear zone; KKSZ=Kanairiktok shear zone; FRIS=Flowers River Igneous Suite; NQO=New Québec orogen.*

provides the highest resolution multispectral satellite data available with 16 spectral bands and a spatial resolution of 2–3.7 m. This enables the identification of key mineral groups and characterization of even small outcrops while reducing spectral interference from vegetation and surficial materials. This study focuses on a key area of the northwestern Hopedale block, the Ingrid Group, the Torngat orogen and portions of the Nain Plutonic Suite (Figure 2). The primary objective is to highlight discrepancies between existing geological maps and remote sensing interpretations, providing an additional layer of information to support ongoing field investigations, rather than generate a standalone geologic map.

Exposed bedrock surfaces in central Labrador exhibit variable weathering, with spectral data reflecting both primary mineralogy and weathering products such as iron oxides, clays and hydroxides. These mineral groups are readily detected by multispectral satellite sensors and serve as proxies for primary mineralogy. Data processing highlights variations in iron (oxy-)hydroxides, derived from the weathering of olivine or sulphides, as well as AlOH-bearing minerals (*e.g.*, muscovite) and general OH-bearing (hydrous) minerals, including clay minerals, micas and amphiboles. As a result, lithological contrasts between mafic and felsic rocks, as well as between rocks with varying hydrous mineral abundances, are well-defined. However, spectral differentiation between compositionally similar lithologies, such as granitoids and quartzofeldspathic orthogneisses, remains problematic.

While the results demonstrate the utility of multispectral satellite data for geological applications in central Labrador, challenges remain, particularly due to cloud cover, atmospheric haze, and the need for ground-truthing to validate spectral interpretations. Future work will incorporate spectral calibration using field samples and explore advanced processing techniques applied to data acquired under more favourable atmospheric conditions, enhancing lithologic classifications and mapping accuracy.

## GEOLOGY

The project covers a 28.5-km long, northwest–southeast transect across the northwestern Hopedale block, Aucoin Plutonic Suite, the Ingrid Group, the Torngat orogen and the Nain Plutonic Suite, within the central portions of UTM grids 13N/05 and 06. The Hopedale block, representing the southern part of the Archean North Atlantic Craton in Labrador, consists of quartzofeldspathic Maggo Gneiss, granitic intrusions of the Kanairiktok Intrusive Suite, and possibly small fragments of the Weekes amphibolite. The Neoarchean Aucoin Plutonic Suite is represented in the study area by syenogranitic to monzogranitic intrusions, including the monzodiorite–syenite body hosting the Aucoin Prospect (Sandeman and McNicoll, 2015).

The Ingrid Group comprises a Paleoproterozoic volcano-sedimentary succession deposited during the final stages of the Torngat orogeny, which represents the easternmost part of the Southeastern Churchill Province. In the study area, the Torngat orogen includes high-grade metamorphic rocks of the Lac Lomier and Tasiuyak complexes. The Nain Plutonic Suite, a Mesoproterozoic anorthosite–mangerite–charnockite–granite (AMCG) suite, consists of monzogranites, leucogabbro to gabbronorite and anorthosites, some of which may be present within the study area. For a more comprehensive geological and tectonic overview, as well as details on ongoing mapping projects, readers are referred to Scorsolini *et al*. (*this volume)*, Hinchey *et al.* (2024) and Sandeman and McNicoll (2015).

### DATA PROCESSING AND RESULTS

The data for this project was acquired as part of the proposal "WorldView-3 supported bedrock mapping in remote areas of Labrador (PP0097103)", submitted to the Earth Observation (EO) division of the European Space Agency. The successful application facilitated the acquisition of multispectral and shortwave infrared data captured by the WorldView-3 satellite system. The 156 km$^2$ project area was divided into three tiles to align with the satellite's flight path, with acquisition occurring on August 14, September 2 and 7, 2024, at 15:13, 15:21 and 15:05 UTC, respectively. The average cloud cover was 14.1% with additional cloud shade in the central tile, and diffuse clouds and haze in the eastern and western tiles (Figure 3A). Key acquisition parameters included solar azimuth between 159 and 165°, sun elevation between 47.3 and 39.2° and off-nadir view angles of 3.5 to 18.7°. The overall data quality is suboptimal, limiting the application of intensity thresholds across illumination gradients produced by haze, as well as advanced processing like spectral unmixing and principal component analyses, which rely on uniform signals across the tiles.

Sixteen spectral bands between 425 and 2330 nm were captured, with a spatial resolution of 2 m for eight visible near infrared (VNIR) bands between 425 and 950 nm, and 3.7 m for eight shortwave infrared (SWIR) bands between 1210 and 2330 nm (Figure 3A–C). A panchromatic band with a 0.5 m resolution was also included. The data was delivered as Level LV3D, orthorectified and radiometrically corrected, 1:12 000 tiled GeoTIFF files.

The data was processed using ENVI 6.1 software. Following import and initial screening, a radiometric calibration to produce Top-of-Atmosphere reflectance was per-

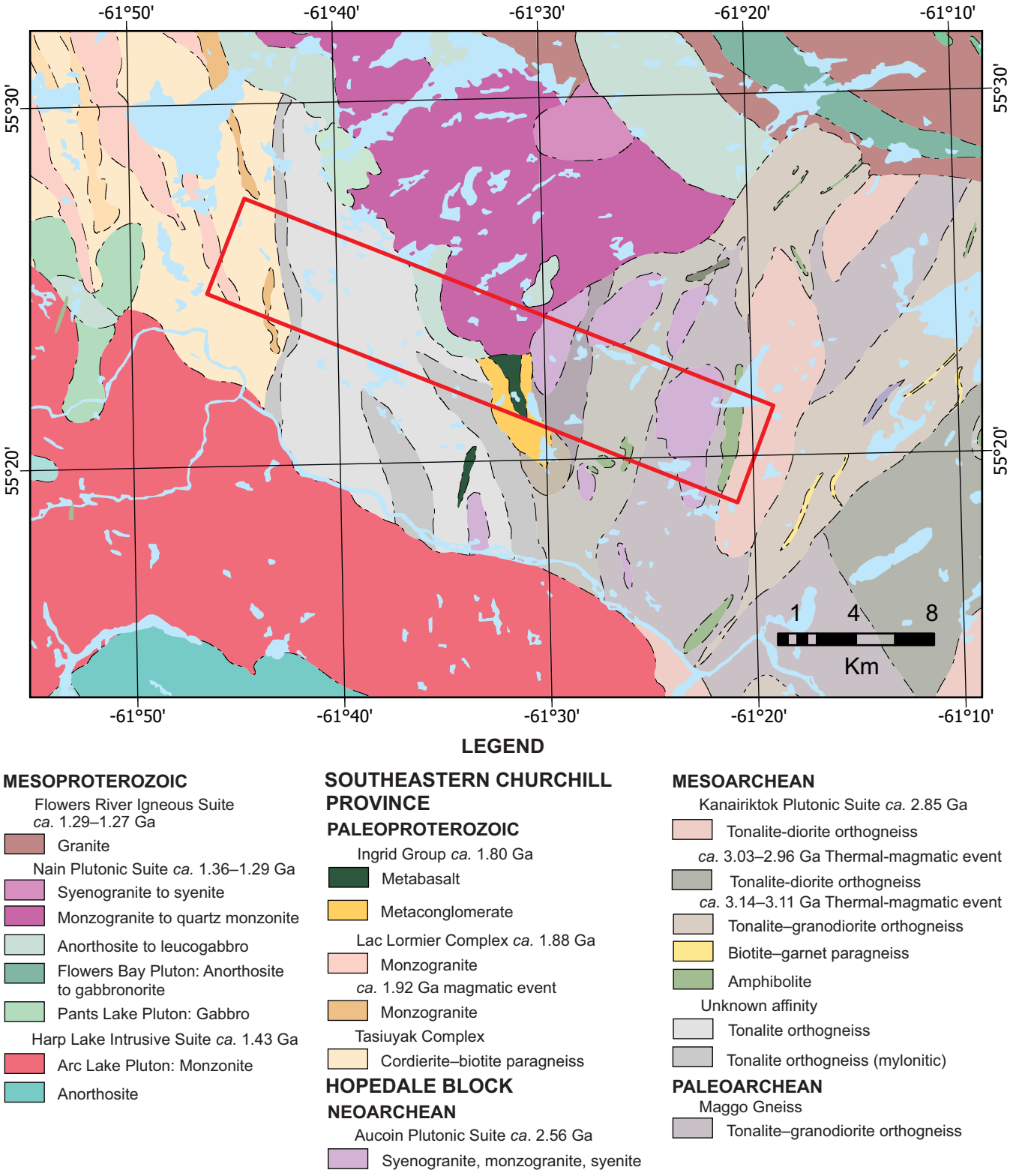


**Figure 2.** *Geologic map of the project area across the boundary of the Hopedale block in the east, Nain Plutonic Suite (north), Harp Lake Intrusive Suite (south) and Southeastern Churchill Province (west, geology from A. Hinchey, unpublished data, 2025). WorldView-3 coverage outlined by the red box also indicates locations of panels A–C in Figure 3.*

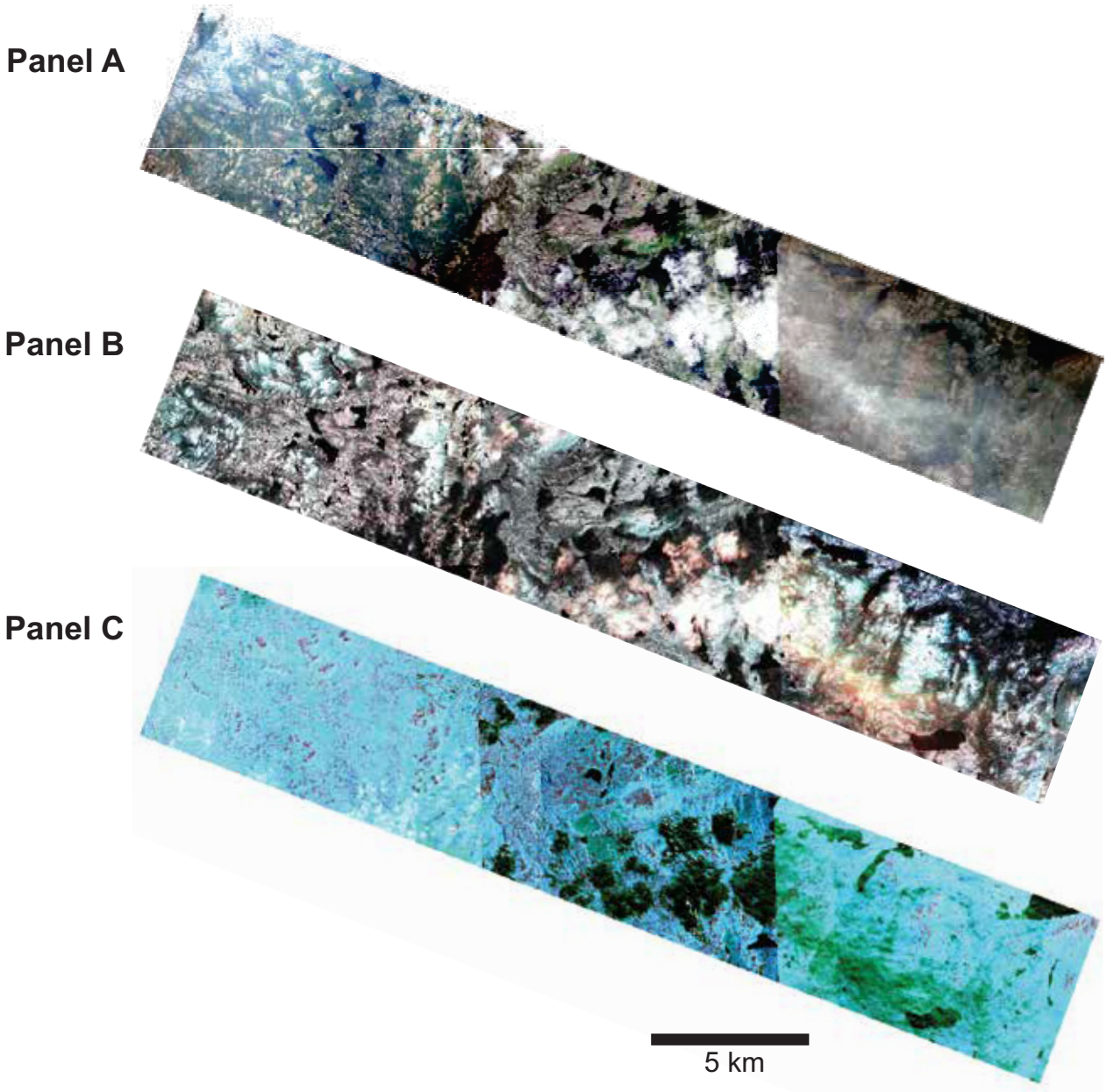


**Figure 3.** *Data from WorldView-3 satellite, provided in three panels and stitched together. Panel A) Natural colour; Panel B) False-colour shortwave infrared bands 3-4-5 composite to highlight bedrock outcrops in pink; Panel C) Results of band ratios to highlight iron hydroxides (red), hydrous minerals (green), and aluminum hydroxide minerals (blue). Clouds, haze, vegetation and lakes produce noise, and green to blue interference colours that were avoided by manually mapping outcrop locations.*

formed. All 16 bands were then stacked, co-registered and resampled to a 2 m resolution. Fast Line-of-Sight Atmospheric Analysis of Hypercubes (FLAASH) correction was then applied to all bands to reduce atmospheric effects and attenuation. However, the presence of haze in the eastern and western tiles was visually more pronounced after atmospheric correction and may require reassessment in future iterations of the dataset processing. Initial attempts to mask clouds and vegetation automatically using band thresholds or unsupervised clustering methods were unsuccessful due to the non-uniform distribution of haze and resulting illumination gradients across tiles. As a result, manual identification and cropping of suitable outcrops were performed.

Band ratios calculated from different spectral bands are a well-established processing method in multispectral analysis, leveraging mineral- or component-specific absorption

features (for a review of satellite multispectral processing methods, *see* van der Meer *et al.*, 2012). This process builds a pixel-by-pixel intensity ratio of bands that capture specific absorption or reflectance features of mineral groups. Three band ratios were selected for this study, based on specific spectral responses (Figure 4A–C, adjusted after Sun *et al.*, 2017):

1) **Iron-hydroxide molecular bonds** occur in minerals like chlorite, amphibole and Fe-rich clays like nontronite (Burns and Strens, 1966). The Fe-OH bond present in chlorite and nontronite produces a characteristic absorption at 2210–2300 nm. Combining ratios of SWIR bands 1, 3 and 7, a higher signal in the result will also identify the presence of ferrihydrite. The band ratio is calculated as:

$$FeOH_{int} = \frac{\text{SWIR3 [1660 nm]}}{\text{SWIR7 [2260 nm]}} * \frac{\text{SWIR3 [1660 nm]}}{\text{SWIR1 [1210 nm]}} \quad \text{Formula 1}$$

2) **Hydrous minerals** such as micas, clays, opal and amphiboles, contain hydroxyl bonds and display absorption features for the O-H bond and metal-OH bonds, particularly around 1400, 1900 and 2200–2300 nm (van der Meer, 2004). The band ratio is calculated as:

$$Hydroxyl_{int} = \frac{\text{SWIR6 [2205 nm]}}{\text{SWIR7 [2260 nm]}} * \frac{\text{SWIR3 [1660 nm]}}{\text{SWIR6 [2205 nm]}} \quad \text{Formula 2}$$

3) **Aluminum-hydroxide-bearing minerals** can be identified by a specific absorption feature around 2170–2210 nm, most prominently developed in muscovite, clays such as kaolinite, dickite, halloysite, montmorillonite, illite and smectite, as well as alunite (van der Meer, 2004). The relative abundance of Al-OH bearing minerals can be calculated as:

$$AlOH_{int} = \frac{\text{SWIR3 [1660 nm]}}{\text{SWIR6 [2205 nm]}} * \frac{\text{SWIR7 [2260 nm]}}{\text{SWIR6 [2205 nm]}} \quad \text{Formula 3}$$

The resulting range of each band ratio was then set to thresholds based on the variation observed in the image areas of bedrock outcrop only. This approach highlights the variation across outcrops by utilizing the full range of contrasts, though it may lead to over- or under-saturation in other areas (Figure 3C). Individually assessing the three tiles yielded a comparable RGB colour range. The three band ratios were then combined into an RGB false-colour image to highlight lithologic changes and track similar spectral responses across outcrops. Six RGB combinations were selected based on the dominant intensities:

– **Red and blue:** Areas of similarly high intensity of the $FeOH_{int}$ and $AlOH_{int}$ band ratios, but lower $Hydroxyl_{int}$.

– **Red and green:** Areas of high intensity of $Hydroxyl_{int}$, intermediate intensity of $FeOH_{int}$ and low $AlOH_{int}$.

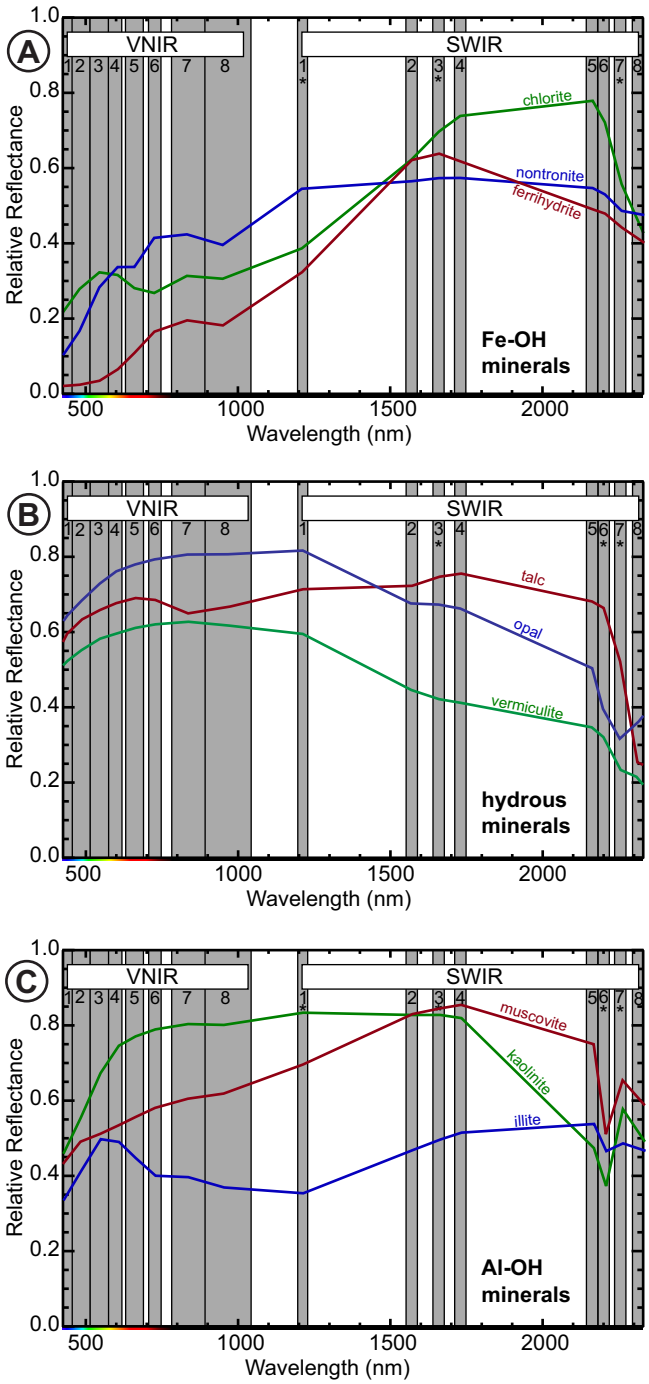


**Figure 4.** *Mineral reflectance modelled to WorldView-3 spectral bands. The eight visible-near infrared bands (VNIR) and eight shortwave infrared bands (SWIR) cover key absorption features of A) Fe-OH minerals; B) Hydrous minerals; C) Al-OH minerals. The SWIR bands used in the corresponding band ratios are indicated by an asterisk. Spectra are modelled to WorldView-3 bandwidths based on the USGS spectral library Version 7 (Kokaly* et al.*, 2017).*

– **Red:** Areas of high intensity of $FeOH_{int}$ and low intensities in the $Hydroxyl_{int}$ and $AlOH_{int}$.

– **Pink:** High intensity of $AlOH_{int}$, intermediate $FeOH_{int}$ and low $Hydroxyl_{int}$.

– **Green and blue (dark):** Low, but similar intensities for all band ratios.

– **Mix:** High variability of intensity combinations over small distances.

These combinations were distinguished and manually mapped, avoiding areas of cloud cover, cloud shade, haze and non-bedrock areas like till cover and vegetation.

## DISCUSSION

Band ratios calculated from WorldView-3 data reflect variations in the abundance of FeOH- and AlOH-bearing minerals, as well as a broader group of hydrous minerals. Based on field observations in the region, these abundances represent the top, millimetre-scale surfaces of exposed bedrock, primarily consisting of surficial weathering products of the original mineralogy. For many of the common lithologies in the area, the spectral FeOH component ($FeOH_{int}$) likely represents the weathering products of ferromagnesian minerals abundant in mafic and ultramafic rocks, such as olivine and pyroxene, leading to the formation of ferrihydrite and nontronite (iddingsite, *cf.* Delvigne *et al.*, 1979; Wilson, 2004). AlOH-bearing minerals ($AlOH_{int}$) such as muscovite/sericite, kaolinite, illite, smectite and other clays, can be part of the original mineralogy, although they are more commonly produced by hydrothermal alteration or surficial weathering of aluminosilicate minerals like K-feldspar and plagioclase (Wilson, 2004, and references therein, Bétard *et al.*, 2009). The broader group of hydrous minerals ($Hydroxyl_{int}$) overlaps with the FeOH- and AlOH-indices but also includes a wider range of MgOH-bearing minerals, as well as hydrous minerals like amphiboles and biotite. This interpretation is supported by spot analyses of spectra modelled against the USGS mineral spectral library Version 7 (Kokaly *et al.*, 2017) in ENVI, which returned ferrihydrite, nontronite, actinolite, muscovite, hornblende, epidote, chlorite, jarosite, hematite and goethite as common mineral species present in varying abundance in many outcrops across the project area. However, results for individual pixels exhibit considerable variability due to atmospheric interference and the spectral sub-library used.

The RGB false-colour image, resulting from the combination of the $FeOH_{int}$, $Hydroxyl_{int}$ and $AlOH_{int}$ in the red, green and blue channels, respectively, provides the basis for a remote predictive map built upon six manually distinguished map units (Figure 5A–C). These units qualitatively indicate underlying bedrock types, inferred from their weathering products. Red regions suggest bedrock rich in olivine, pyroxene, or other ferromagnesian silicates that are labile at the surface, green regions indicate rocks rich in hydrous minerals such as biotite, amphibole, and labile aluminosilicates, and blue regions point to rocks high in muscovite and general aluminosilicates. These interpretations of classes and their corresponding unweathered mineralogy remain tentative and require ground-truthing. Additionally, they need to be evaluated for interferences, such as the presence of till, which has been filtered out visually but remains spectrally indistinguishable from bedrock. However, till in the area comprises less than 10% clays (H. Campbell, pers. comm., 2024), hence its impact on the spectral signal may be minimal.

Lithologic variations identified through multispectral satellite data largely align with the mapped units and mineralogical variability within these units across the project area. Notable examples of confirmed lithologic contacts include the well-studied Aucoin Plutonic Suite in the eastern portion of the project area and the contact between a north–south striking occurrence of mylonitic orthogneiss and tonalitic orthogneiss in the western part of the project area. The multispectral data captures the lithologic variability within the volcano-sedimentary succession of the Ingrid Group, showing a range of signal combinations over short distances.

In areas where multispectral results deviated from the currently mapped units, such as a group of outcrops in the northwestern part of the project area, the presence of an undifferentiated unit of orthopyroxene-, clinopyroxene-, hornblende-, biotite- and garnet-bearing migmatitic tonalitic orthogneiss, which also contains amphibolite pods (A. Hinchey, unpublished data, 2025), resulted in significant variability in multispectral signals. This variability is unsurprising for such a complex, composite unit, and the results presented here offer valuable information that could assist in subdividing the unit. Additionally, in the central project area, to the north of the Ingrid Group, monzogranite or monzonite of the Nain Plutonic Suite is currently undifferentiated in the latest map. The multispectral data suggests the presence of a distinct contact between at least two lithologies. The contrast observed here is likely due to a change in the relative intensity of the $AlOH_{int}$ signal, possibly reflecting an increased abundance of anorthite, which readily weathers to clay. This could indicate the presence of an anorthosite intrusion, potentially similar to one mapped less than a kilometre to the northeast.

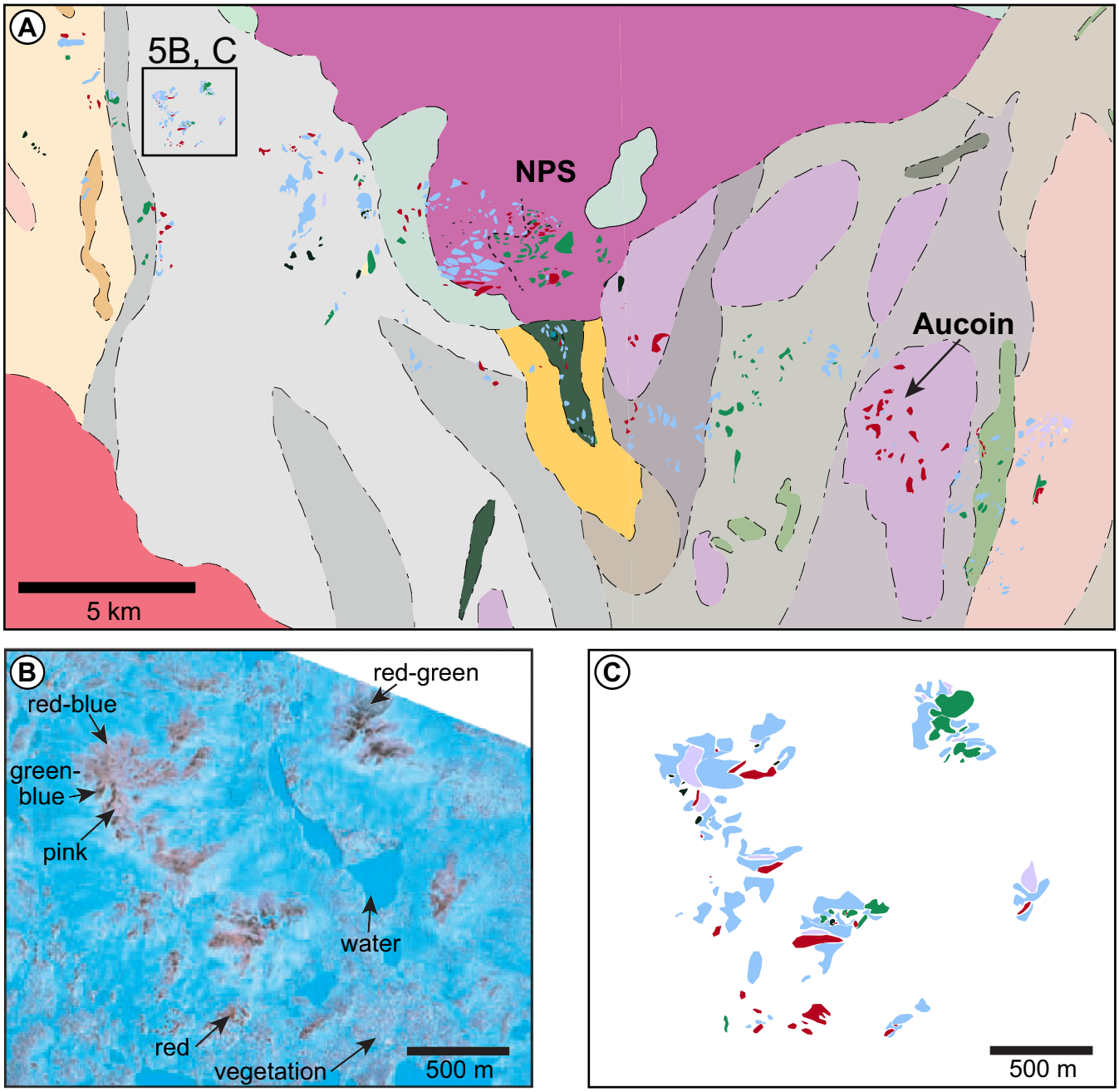


**Figure 5.** *Spectral results mapped as six classes of distinct spectral responses. A) Spectral classes overlain on the geologic map from Figure 2 highlight areas of good agreement in the east around the Aucoin prospect. The remote sensing results indicate additional complexity in areas like the southern Nain Plutonic Suite.* See *Figure 2 for bedrock geology legend. Geology after A. Hinchey (unpublished data, 2025). A potential contact between currently undifferentiated lithologies is indicated by the dashed line. Panels B and C highlight an area of complexity in an undifferentiated unit mapped as orthogneiss of uncertain affinity. Examples of spectral response combinations are indicated.*

## FUTURE RESEARCH

The preliminary results presented here will be used to guide fieldwork, which will allow for the ground-truthing of remote predictive maps. This iterative process will help improve the accuracy of outcomes and assess potential biases, such as the influence of vegetation and lichen cover, which may preferentially develop over felsic and alkaline bedrock and attenuate signals. The weathering products and associated unweathered mineralogy will need to be tested through in-situ spectral analysis of both weathering rinds and fresh underlying surfaces. Furthermore, the depth and intensity of weathering may be more advanced in olivine-bearing and non-siliceous lithologies, leading to higher abundances of minerals that produce better spectral responses compared to weathering-resistant quartz-rich rocks, introducing a potential bias. Illumination and attenuation gradients caused by haze, cloud, or cloud shade were assessed manually, but rigorous quality control measures are needed to ensure the robustness of the resulting interpretations. The suboptimal atmospheric conditions during data capture rendered intensity thresholds, supervised and unsupervised clustering methods, and machine learning applications impractical for this dataset. These advanced processing methods will instead be applied to other datasets for the region, such as ASTER and Sentinel-2 multispectral images, and the potential re-capture of the area by WorldView-3 under improved weather conditions. Multispectral and satellite radar data used to assess surface roughness will be combined with additional geophysical information to evaluate the continuity of units at depth and across covered areas.

## CONCLUSIONS

WorldView-3 satellite multispectral data enabled the identification of six distinct types of bedrock lithologies in the project area and their distribution in a key tectonic region between the Hopedale block and the Southeastern Churchill Province in central Labrador. The resulting remote predictive map generally agrees with existing bedrock maps but also identifies areas of additional complexity and updated contact locations, particularly within generalized composite units comprising different rock types. These findings underscore the value of remote sensing datasets for bedrock mapping in central Labrador, while also highlighting the limitations of datasets acquired under non-ideal atmospheric conditions and the necessity of ground-truthing to validate and iteratively improve remote sensing results.

## ACKNOWLEDGMENTS

The satellite data utilized in this project were provided through ESA project PP0097103, supported by the European Space Agency and European Space Imaging. Special thanks are extended to Thierry Büttel and the team at EUSI for their invaluable support and guidance throughout the acquisition process.

## REFERENCES

Bétard, F., Caner, L., Gunnell, Y. and Bourgeon, G.
2009: Illite neoformation in plagioclase during weathering: Evidence from semi-arid Northeast Brazil. Geoderma, Volume 152, Issues 1-2, pages 53-62.

Burns R.G. and Strens, R.G.J.
1966: Infrared study of the hydroxyl bands in clinoamphiboles. Science, Volume 153, pages 890-892.

Delvigne, J, E., Bisdom, B. A., Sleeman J. and Stoops G.
1979: Olivines, their pseudomorphs and secondary products. Pedologie, Volume 29, pages 247-309.

Di Tommaso, I. and Rubinstein, N.
2007: Hydrothermal alteration mapping using ASTER data in the Infiernillo porphyry deposit, Argentina. Ore Geology Reviews, Volume 32, pages 275-290.

Hinchey, A.M., Rayner, N., Diekrup, D., Sandeman, H.A.I. and Mendoza Marin, D.
2024: New U–Pb shrimp age constraints on the geodynamic evolution of the Hopedale Block, labrador: Implications for the assembly of the North Atlantic Craton. *In* Current Research. Government of Newfoundland and Labrador, Department of Industry, Energy and Technology, Geological Survey, Report 24-1, pages 155-180.

Kruse, F.A., Baugh, W.M. and Perry, S.L.
2015: Validation of DigitalGlobe WorldView-3 Earth imaging satellite shortwave infrared bands for mineral mapping. Journal of Applied Remote Sensing, Volume 9, Issue 1. https://doi.org/10.1117/1.JRS.9.096044

Pour, A.B., Hashim, M., Hong, J.K. and Park, Y.
2019: Lithological and alteration mineral mapping in poorly exposed lithologies using Landsat-8 and ASTER satellite data: North-eastern Graham Land, Antarctic Peninsula. Ore Geology Reviews, Volume 108, pages 112-133.

Kokaly, R.F., Clark, R.N., Swayze, G.A., Livo, K.E., Hoefen, T.M., Pearson, N.C., Wise, R.A., Benzel, W.M., Lowers, H.A., Driscoll, R.L. and Klein, A.J.
2017: USGS Spectral Library Version 7. United States Geological Survey, Data Series, Volume 1035, 61 pages.

Sandeman, H.A.I. and McNicoll, V.J.
2015: Age and petrochemistry of rocks from the Aucoin gold prospect (NTS map area 13N/6) Hopedale block, Labrador: Late Archean, alkali monzodiorite-syenite hosts Proterozoic orogenic Au–Ag–Te mineralization. *In* Current Research. Government of Newfoundland and Labrador Department of Natural Resources, Geological Survey, Report 15-1, pages 85-103.

Scorsolini, L.G., Hinchey, A.M. and Diekrup, D.
*This volume*: Deformation, metamorphism and magmatic activity in the southern Torngat Orogen, Labrador.

Sparkes, G.W., Hinchey, J.G. and Diekrup, D.
2023: WorldView-3 satellite imagery as a tool for hydrothermal alteration-mineral mapping: Insights from the Long Harbour Group, Avalon Zone, Newfoundland. *In* Current Research. Government of Newfoundland and Labrador, Department of Industry, Energy and Technology, Geological Survey, Report 23-1, pages 127-142.

Sun, Y., Tian, S. and Di, B.
2017: Extracting mineral alteration information using WorldView-3 data. Geoscience Frontiers, Volume 8, Issue 5, pages 1051-1062.

van der Meer, F.
2004: Analysis of spectral absorption features in hyperspectral imagery. International Journal of Applied Earth Observation and Geoinformation, Volume 5, Issue 1, pages 55-68.

van der Meer, F.D., van der Werff, H.M., van Ruitenbeek, F.J., Hecker, C.A., Bakker, W.H., Noomen, M.F., van der Meijde, M., Carranza, E.J.M., De Smeth, J.B. and Woldai, T.
2012: Multi-and hyperspectral geologic remote sensing: A review. International Journal of Applied Earth Observation and Geoinformation, Volume 14, Issue 1, pages 112-128.

Wilson, M.J.
2004: Weathering of the primary rock-forming minerals: Processes, products and rates. Clay Minerals, Volume 39, Issue 3, pages 233-266.